Journal of Sound and Vibration (2000) **237**(3), 457–475
doi:10.1006/jsvi.2000.3066, available online at http://www.idealibrary.com on IDEAL®

TIME-SEGMENTED FREQUENCY-DOMAIN ANALYSIS FOR NON-LINEAR MULTI-DEGREE-OF-FREEDOM STRUCTURAL SYSTEMS

W. J. Mansur and J. A. M. Carrer

Department of Civil Engineering, COPPE/Federal University of Rio de Janeiro, CEP 21945-970, *Rio de Janeiro C.P.* 68506, *RJ, Brazil. E-mail: webe@coc.ufrj.br*

W. G. Ferreira

Technological Center, Federal University of Espirito Santo, Vitoria, Brazil

A. M. Claret de Gouveia

School of Mines, Federal University of Ouro Preto, Ouro Preto, Brazil

and

F. Venancio-Filho

Department of Applied Mechanics and Structures, Federal University of Rio de Janeiro, Rio de Janeiro, Brazil

(*Received* 30 *August* 1999, *and in final form* 24 *April* 2000)

This paper presents a new frequency-domain method to analyze physically non-linear structural systems having non-proportional damping. Single- and multi-degree-of-freedom (d.o.f.) systems subjected to time-dependent excitations are considered. A procedure to consider initial conditions, required by the methodology described, is discussed. The algorithm described here employs a time-segmented procedure in modal co-ordinates in the frequency domain; solution in each time-segment being obtained by an iterative process. The proposed methodology is validated by three examples. The procedure presented here can be employed as well to analyze structural systems with viscous and hysteretic damping or else with frequency-dependent damping properties.

1. INTRODUCTION

Dynamic non-linear analyses are usually performed in the time-domain by direct integration of the equations of motion in physical co-ordinates. The so-called mode superposition method has also been used as an alternative time-domain procedure, where modal co-ordinates are employed instead of the physical ones. However, when the structural system has hysteretic damping or frequency-dependent damping characteristics, the analysis in frequency domain is more adequate.

In recent years, a number of procedures have been presented for non-linear analyses in the frequency domain. Kawamoto [1] proposed a hybrid time-frequency method where the original system is replaced by a pseudo-linear system; the equations of motion being solved in the frequency domain, and the non-linear contribution being dealt with in the time-domain through the pseudo-force method. Aprile *et al.* [2] generalized

0022-460X/00/430457 + 19 $35.00/0

Kawamoto's procedure making it possible to consider hysteretic and frequency-dependent damping.

Itoh [3] presented a frequency-domain procedure to obtain responses of systems with non-proportional damping where he makes use of a complex modal basis to uncouple the equations of motion. The final algorithm employs only real algebra, and does not take advantage of some characteristics of the classical mode superposition method.

Chen and Taylor [4] proposed uncoupling the dynamic equilibrium equations for systems with non-proportional damping, through a basis composed by Ritz vectors instead of the complex modal basis. Chang and Mohraz [5] used the mode superposition method to deal with physically non-linear structural systems with non-proportional damping; they established an iterative procedure through Taylor series expansions.

Claret and Venancio-Filho [6] considered non-proportional damping via the pseudo-force concept. The pseudo-force formulation led to an iterative process, which was solved in the time-domain via Duhamel integral. The convergence of the iterative process was quite good. Jangid and Datta [7] employed the same procedure as Claret and Venancio-Filho; however the iterative process was performed in the frequency domain.

The present work is concerned with a discussion aiming at generalizing existing frequency-domain procedures for non-linear structural systems with non-proportional damping. A new and quite general methodology to consider physical non-linearities is presented, making it possible to consider structural damping. The solution of either linear or non-linear single-degree-of-freedom (s.d.o.f.) systems is obtained by the matrix formulation presented by Venancio-Filho and Claret [8], namely the implicit Fourier transform (ImFT). It is important to mention that concerning the non-linear formulation initial conditions are considered as described by Ferreira *et al.* [9] and that the procedure presented in that paper is herein generalized to consider multi-degree-of-freedom systems. In order to obtain the time-history of the response for non-linear s.d.o.f. or m.d.o.f. systems with non-proportional damping, a time segmentation technique is employed over modal co-ordinates. The coefficients responsible for coupling are considered as pseudo-forces, thus an iterative procedure naturally arises.

2. LINEAR SINGLE-DEGREE-OF-FREEDOM SYSTEMS

The equation of motion for an s.d.o.f. system with viscous damping is given by

$$m\ddot{v}(t) + c\dot{v}(t) + kv(t) = p(t), \tag{1}$$

where m, c and k are, respectively, mass, damping and stiffness coefficients, and v is the mass displacement.

The time-domain solution of equation (1) can be obtained through the following inverse discrete Fourier transform (iDFT) formula:

$$v(t_n) = \frac{\Delta\bar{\omega}}{2\pi} \sum_{m=0}^{N-1} H(\bar{\omega}_m) P(\bar{\omega}_m) \mathrm{e}^{mn(\mathrm{i}(2\pi/N))} \tag{2}$$

where $P(\bar{\omega}_m)$ is the discrete Fourier transform (DFT) of $p(t)$, i.e.,

$$P(\bar{\omega}_m) = \Delta t \sum_{n=0}^{N-1} p(t_n) \mathrm{e}^{-mn(\mathrm{i}(2\pi/N))} \tag{3}$$

i is the complex unit, N is the number of sampling points, $t_n = n\Delta t$, are the discrete times, $\Delta t = T_p/N$ is the time interval in which the sampling time T_p is subdivided. T_p is also referred to as extended period and $\bar{\omega}_m = m\Delta\bar{\omega}$ are the discrete frequencies, where $\Delta\bar{\omega} = 2\pi/T_p$. $H(\bar{\omega}_m)$ is the complex frequency response function (CFRF) at the discrete frequency $\bar{\omega}_m$, i.e.,

$$H(\bar{\omega}_m) = \begin{cases} \dfrac{1}{-\bar{\omega}_m^2 m + k + \mathrm{i}\bar{\omega}_m c} & \text{for } m \leqslant N/2, \\ \text{conjugate}[(H(\bar{\omega}_{N-m}))] & \text{for } m > N/2. \end{cases} \tag{4}$$

It is important to notice that the spectrum of $v(t)$,

$$V(\bar{\omega}_m) = H(\bar{\omega}_m)P(\bar{\omega}_m), \tag{5}$$

is available to the engineer (see equation (2)) when the standard DFT algorithm described above is employed.

The linear viscous damping model (see equation (1)) is currently adopted because it leads to a convenient solution of the equation of motion and it can be adjusted to yield reasonable results as long as damping is not too high. However, its use in structural dynamics is at least conceptually incorrect as viscous-damping modelling leads to frequency-dependent energy dissipation for harmonic motions, i.e., the damped system behaves in a way which lacks experimental support. Thus, in what concerns structural damping, whenever possible one should use a model whose energy dissipation is not frequency dependent. Such a model is the so-called hysteretic damping model, for which the CFRF for the s.d.o.f. system can be expressed as

$$H(\bar{\omega}_m) = \frac{1}{-\bar{\omega}_m^2 m + k(1 + \mathrm{i}\lambda)}, \tag{6}$$

$\lambda = 2\xi$ being the hysteretic damping factor and ξ being the damping ratio [10].

The discrete time-history of displacement obtained by the DFT procedure as shown by equations (2) and (3), can be alternatively obtained by a unique matrix operation

$$\mathbf{v} = \frac{1}{N}\,\mathbf{ep}, \tag{7}$$

where $\mathbf{v}$ is a vector describing the mass displacement time-history whose entries v_n are equal to $v(t_n)$, $\mathbf{p}$ is the discrete loading vector whose entries are $p_n = p(t_n)$. As all operations required to perform the DFT and the iDFT are implicitly considered by matrix $\mathbf{e}$, it is called the implicit Fourier transform matrix. The following matrix product obtains the entries of matrix $\mathbf{e}$:

$$\mathbf{e} = \mathbf{EHE}^*, \tag{8}$$

where $\mathbf{E}^*$ carries out in matrix form the DFT operation indicated by equation (3), i.e., $\mathbf{P} = \Delta t\mathbf{E}^*\mathbf{p}$, $\mathbf{P}$ being a vector whose entries are $P_n = P(\bar{\omega}_m)$. $\mathbf{E}^*$ entries are given by

$$E^*_{m+1,n+1} = \mathrm{e}^{-mn(\mathrm{i}(2\pi/N))} \tag{9}$$

$\mathbf{E}$ carries out in matrix form the iDFT operation indicated by equation (2), i.e., $\mathbf{v} = (\Delta\bar{\omega}/2\pi)\mathbf{EHP}$, $\mathbf{H}$ being a diagonal matrix whose entries are $H_{m+1,m+1} = H(\bar{\omega}_m)$.

E entries are given by

$$E_{m+1,n+1} = e^{mn(i(2\pi/N))}, \tag{10}$$

i.e., $E_{m+1,n+1} = \text{conj}(E^*_{m+1,n+1})$.

The discrete time-history of velocities can be computed as indicated by Ferreira [11] and Ferreira *et al.* [9].

Now, one of the advantages of using the implicit Fourier transform (ImFT) algorithm described above (see equation (7)) appears at full extent. If the number of Fourier coefficients is large enough to yield accurate time response for **v** as expressed by equation (7) and the extended period is large enough, causality should be obeyed, i.e., a discrete value of $p(t_j)$ should not contribute to a discrete value of $v(t_i)$ whenever $j > i$. Thus, if one is interested only in the first S terms of the response, only the coefficients e_{ij} such that $i \leqslant S$, $i > j$, need to be considered. Such a reduced **e** $(S \times S)$ lower triangular matrix can be generated by the complete **H** $(N \times N)$ matrix and by reduced **E** $(S \times N)$ and **E*** $(N \times S)$ matrices. The causality property described above will prove to be very useful in the scheme for non-linear analysis presented in this paper where a lower triangular **e** $(S \times S)$ matrix together with reduced $(S \times 1)$ **p** and **v** vectors are considered rather than a complete **e** $(N \times N)$ matrix and complete $(N \times 1)$ **p** and **v** vectors. One must also notice that the e_{ij} coefficients have a number of properties as described by Ferreira [11] which if taken into consideration lead to substantial savings in the assemblage of the **e** matrix. An important characteristic of matrix **e** which must be observed is that **e** is a Toeplitz matrix, i.e., $e_{i+k,j+k} = e_{i,j}$). Thus, only its first column has to be calculated.

3. INITIAL CONDITIONS

Aiming at performing a time-segmented non-linear analysis, where displacement and velocity at the end of one segment are used as initial conditions for the subsequent segment, a procedure to include initial displacement and velocity is discussed next.

The time response due to an initial displacement v_0 can be obtained by adding to a constant in time displacement v_0, the effect of a force $-f_0$:

$$\mathbf{v} = \frac{1}{N}\mathbf{e}(-f_0\mathbf{1}) + v_0\mathbf{1}, \tag{11}$$

where **1** is a vector of order $(S \times 1)$, whose elements are equal to unity and f_0 is the static force on the spring due to the displacement v_0. If the analysis is linear elastic, then $f_0 = k_0 v_0$, if it is non-linear, f_0 must be obtained from the load $\times$ displacement diagram for the spring.

The response corresponding to an initial velocity $\dot{v}_0$ is the same as that due to an impulse of intensity $m\dot{v}_0$, which can be obtained from

$$v(t) = m\dot{v}_0 h(t), \tag{12}$$

where $h(t)$ is the unit-impulse response function, i.e., it is the response of the s.d.o.f. system to a unit impulse. From equation (12) one can obtain the discrete time-history displacement vector [9,11] corresponding to an initial velocity $\dot{v}_0$,

$$\mathbf{v} = \frac{1}{N\Delta t} m\dot{v}_0 \mathbf{e}\boldsymbol{\delta}, \tag{13}$$

where $\boldsymbol{\delta}$ is a vector of order $(S \times 1)$ whose first element is unity and all others are null.

When both initial displacement and velocity are considered, one finally arrives at the following expression, which can be used in a time-segmented analysis:

$$\mathbf{v} = \frac{1}{N}\mathbf{e}\left(\mathbf{p} - f_0\mathbf{1} + \frac{m\dot{v}_0}{\Delta t}\boldsymbol{\delta}\right) + v_0\mathbf{1}. \tag{14}$$

4. SINGLE-DEGREE-OF-FREEDOM NON-LINEAR SYSTEMS

Consider a non-linear s.d.o.f. system, whose spring force–deflection relation follows the bilinear law shown in Figure 1.

During the time-marching process, the equilibrium equation may correspond either to segment A–B or B–C. When the time-marching process starts, the analysis is carried out within segment A–B with null initial conditions. The equation of motion then reads

$$m\ddot{v} + c\dot{v} + k_0 v = p \tag{15}$$

and the time response can be obtained from

$$\mathbf{v} = \frac{1}{N}\mathbf{e}\mathbf{p} \tag{16}$$

For segment B–C, the equation of motion reads [12]

$$m\ddot{v}_n + c\dot{v}_n + k_1 v_n = p_n - f_0, \tag{17}$$

where $v_n = v - v_0$, v is the total displacement within segment B–C at time t, and v_0 is the displacement at the end of segment A–B. f_0 ($f_0 = k_0 v_0$) is the external reaction force resulting from a static analysis when the mass is subjected to the displacement v_0. Figure 1 shows that

$$k_1 = k_0 - \Delta k. \tag{18}$$

Considering equations (17) and (18) the following expression can be derived:

$$m\ddot{v}_n + c\dot{v}_n + k_0 v_n = p_n + \Delta k v_n - f_0. \tag{19}$$

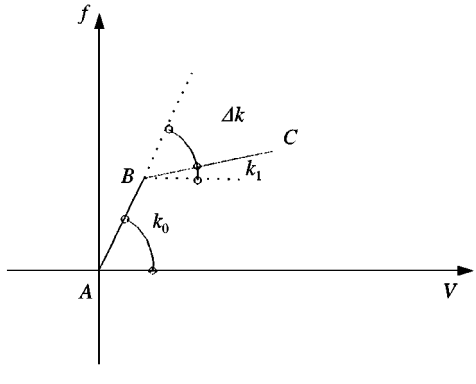

Figure 1. Bilinear force-deflection diagram.

m, c and k_0 on the left hand side (l.h.s.) of equation (19) are the same as for the linear segment A–B (see equation (15)) and the term $\Delta k v_n$ which corresponds to the spring stiffness change, is in fact considered as a pseudo-force, as it now appears on the right hand side (r.h.s.) of equation (19). The iterative procedure employed to solve equation (19) can be described by equation (20), which represents the equation of motion for iteration k:

$$m\ddot{v}_n^{(k)} + c\dot{v}_n^{(k)} + k_0 v_n^{(k)} = p_n + \Delta k v_n^{(k-1)} - f_0. \tag{20}$$

The displacement time-history can then be obtained from

$$\mathbf{v}^{(k)} = \mathbf{v}_n^{(k)} + \mathbf{v}_0\mathbf{1}, \qquad \mathbf{v}_n^{(k)} = \frac{1}{N}\,\mathbf{e}\left(\mathbf{p}_n - f_0\mathbf{1} + \frac{m\dot{v}_0}{\Delta t}\,\boldsymbol{\delta} + \Delta k \mathbf{v}_n^{(k-)}\right), \tag{21}$$

where the contribution of initial velocity has also been included. It should be noticed that the implicit Fourier transform matrix $\mathbf{e}$ is that of segment A–B, i.e., it need not be recalculated.

The iterative process is stopped when

$$\left|\frac{v_{max}^{(k)} - v_{max}^{(k-1)}}{v_{max}^{(k)}}\right| \leqslant \varepsilon, \tag{22}$$

ε being a given tolerance.

Figure 2 illustrates a typical bilinear force–deflection diagram and the mass displacement time-history, corresponding to a segmented analysis with five segments: O–A; A–B; B–C, C–D, D–. The end of the analysis shown in Figure 2 is on the fifth segment where the mass oscillates until it stops. The initial conditions are shown in Table 1.

5. MULTI-DEGREE-OF-FREEDOM LINEAR SYSTEMS

The equation of motion for a viscously damped m.d.o.f. system can be written as

$$\mathbf{m}\ddot{\mathbf{v}}(t) + \mathbf{c}\dot{\mathbf{v}}(t) + \mathbf{k}\mathbf{v}(t) = \mathbf{p}(t), \tag{23}$$

where $\mathbf{m}$, $\mathbf{c}$ and $\mathbf{k}$ are, respectively, mass, damping and stiffness matrices.

Equation (23) can be transformed to modal co-ordinates $\mathbf{Y}(t)$ as

$$\mathbf{I}\ddot{\mathbf{Y}}(t) + \mathbf{C}\dot{\mathbf{Y}}(t) + \boldsymbol{\Lambda}\mathbf{Y}(t) \sim \mathbf{P}(t), \tag{24}$$

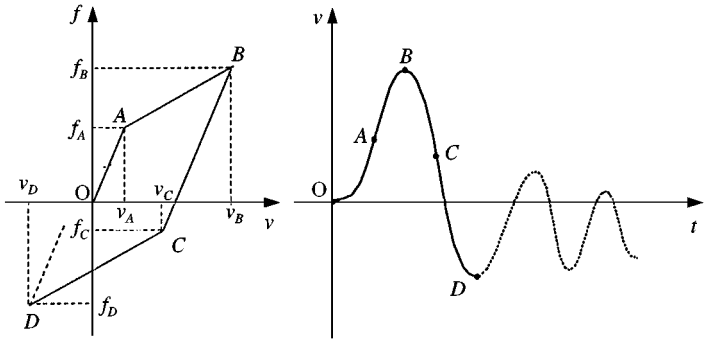

Figure 2. Bilinear force–deflection diagram and time-history of the mass displacement.

TABLE 1

Segmentation analysis sequence and initial conditions for each segment indicated in Figure 2

Segment	Initial conditions		
O–A	$f_0 = 0$	$v_0 = 0$	$\dot{v}_0 = 0$
A–B	$f_0 = f_A$	$v_0 = v_A$	$\dot{v}_0 = \dot{v}_A$
B–C	$f_0 = f_B$	$v_0 = v_B$	$\dot{v}_0 = \dot{v}_B$
C–D	$f_0 = f_C$	$v_0 = v_C$	$\dot{v}_0 = \dot{v}_C$
D–	$f_0 = f_D$	$v_0 = v_D$	$\dot{v}_0 = \dot{v}_D$

where $\mathbf{v}(t) = \mathbf{\Phi Y}(t)$ and $\mathbf{P}(t) = \mathbf{\Phi}^{\mathrm{T}}\mathbf{p}(t)$. $\mathbf{\Phi}$ is the modal matrix normalized with respect to the mass matrix, thus $\mathbf{I}$ in equation (24) is a diagonal unitary mass matrix, $\mathbf{\Lambda}$ is diagonal and $\mathbf{C}$ will be diagonal if $\mathbf{c}$ is proportional, i.e., $\mathbf{c} = a_0\mathbf{m} + a_1\mathbf{k}$.

When the damping matrix $\mathbf{c}$ is proportional the system of equations given by equation (24) is uncoupled and the solution for a modal co-ordinate $\mathbf{Y}_j$, when initial conditions are null, can be obtained from

$$\mathbf{Y}_j = \frac{1}{N}\,\mathbf{e}_j\mathbf{P}_j, \tag{25}$$

where

$$\mathbf{e}_j = \mathbf{E}\mathbf{H}_j\mathbf{E}^*. \tag{26}$$

$\mathbf{H}_j$ is a diagonal matrix whose diagonal coefficients $(\mathbf{H}_j)_{m+1,m+1}$ are given by

$$H_j(\bar{\omega}_m) = 1/[-\bar{\omega}_m^2 + \mathrm{i}\bar{\omega}_m C_{jj} + (1 + \mathrm{i}\lambda)\omega_j^2] \tag{27}$$

and ω_j is the jth natural frequency obtained from the solution of the equation $[\mathbf{k} - \omega^2\mathbf{m}]\mathbf{v} = \mathbf{0}$.

The time response for the physical co-ordinates can be computed from

$$\mathbf{v}(t) = \mathbf{\Phi Y}(t), \tag{28}$$

6. NON-LINEAR MULTI-DEGREE-OF-FREEDOM SYSTEMS WITH PROPORTIONAL DAMPING

The procedure followed for non-linear m.d.o.f. systems is similar to that explained previously for s.d.o.f. systems. The solution process starts on the first segment (linear) for which the procedure indicated by equations (23)–(28) holds.

When the non-linear term responsible for the change in stiffness is considered as pseudo-force, as before, an iterative process arises, and the equilibrium equation for the kth iteration reads

$$\mathbf{m}\ddot{\mathbf{v}}_n^{(k)} + \mathbf{c}\dot{\mathbf{v}}_n^{(k)} + \mathbf{k}_0\mathbf{v}_n^{(k)} = \mathbf{p}_n + \Delta\mathbf{k}\mathbf{v}_n^{(k-1)} - \mathbf{f}_0, \tag{29}$$

where $\mathbf{k}_0$ is the stiffness matrix corresponding to the first segment. As the matrices on the l.h.s. of equation (29) are the same as those shown in equation (23), with $\mathbf{k}_0$ instead of $\mathbf{k}$, the same modal matrix of the linear segment (first segment) can be used to uncouple equations

(29). However, the eigenvalues of the first segment are not orthogonal to the incremental matrix $\Delta\mathbf{k}$, consequently the modal incremental matrix $\mathbf{K}_N = \mathbf{\Phi}^{\mathrm{T}}\Delta\mathbf{k}\mathbf{\Phi}$ will have coupled modal coefficients.

Thus, the modal displacement time-history corresponding to equation (29) can be found through the following iterative expressions:

$$\mathbf{Y}_j^{(k)} = \mathbf{Y}_{nj}^{(k)} + Y_{0j}\mathbf{1},$$

$$\mathbf{Y}_{nj}^{(k)} = \frac{1}{N}\mathbf{e}_j\left(\mathbf{P}_{nj} - F_{0j}\mathbf{1} + \frac{\dot{Y}_j}{\Delta t}\boldsymbol{\delta} + \sum_{p=1}^{NGL} K_{Njp}\mathbf{Y}_{np}^{(k-1)}\right) \tag{30}$$

where F_{0j} is the modal reaction which appears on the generalized mass j when the mechanical system is subjected to a static displacement field corresponding to the initial displacement of the current segment and $\dot{Y}_{0j}$ is the corresponding initial modal velocity.

In order to further clarify how F_{0j} is evaluated in a numerical algorithm such as that described in this paper, consider a m.d.o.f. system having only one non-linear spring whose displacement–deflection curve is shown in Figure 2. Concerning the discussion that follows it is instructive to label segments O–A, B–C and D–E as linear and to label segments A–B and C–D as non-linear.

In order to compute the time response for the C–D segment, the displacement and velocities of point C of segment B–C are taken as initial conditions for segment C–D. Thus, F_{0j} is given by

$$F_{0j} = F_j^a + \Lambda_{0j}\Delta Y_{0j} \tag{31}$$

where Λ_{0j} is the jth diagonal coefficient of the modal stiffness matrix $\mathbf{\Lambda}_0 = \mathbf{\Phi}^{\mathrm{T}}\mathbf{k}_0\mathbf{\Phi}$ and ΔY_{0j} is the incremental modal displacement of the generalized mass j at the end of the segment B–C. $\Lambda_{0j}\Delta Y_{0j}$ is an incremental modal static linear elastic force on the generalized mass j and F_j^a represents static force contributions due to previous segments.

As the procedure is segmented, the next step consists in finding the response for segment D–E. The final conditions of segment C–D are now the initial conditions for segment D–E. In this case, F_{0j} for segment D–E reads

$$F_{0j} = F_j^a + \varphi_j^{\mathrm{T}}\mathbf{k}_1\mathbf{v}_n \tag{32}$$

where φ_j is the jth eigenvector and $\mathbf{v}_n$ is the incremental displacement vector of the masses at the end of the non-linear segment C–D, expressed in physical co-ordinates. Therefore, $\varphi_j^{\mathrm{T}}\mathbf{k}_1\mathbf{v}_n$ is the incremental modal static force at the generalized mass j that corresponds to the end of the segment C–D, and F_j^a is equal to F_{0j} given by equation (31). Thus, the following general expression can be written:

$$F^a = \sum_a [\Lambda_{0j}\Delta Y_{0j}]^a + \sum_b [\varphi^{\mathrm{T}}\mathbf{k}_1\mathbf{v}_n]^b, \tag{33}$$

where the summations account for contributions of previous steps, both linear ($\sum_a [\Lambda_{0j}\Delta Y_{0j}]^a$) and non-linear ($\sum_b [\varphi^{\mathrm{T}}\mathbf{k}_1\mathbf{v}_n]^b$).

7. NON-LINEAR MULTI-DEGREE-OF-FREEDOM SYSTEMS WITH NON-PROPORTIONAL DAMPING

When the damping is non-proportional the damping modal matrix is not diagonal, thus the analysis in modal co-ordinates is coupled. In this case, the pseudo-force concept is also

used and the coefficients of the modal damping matrix responsible for mode coupling are transferred to the r.h.s. of the modal system of equations. In order to accomplish this task the modal damping matrix $\mathbf{C} = \mathbf{\Phi}^{\mathrm{T}}\mathbf{c}\mathbf{\Phi}$ must be written as

$$\mathbf{C} = \mathbf{C}_D + \mathbf{C}_F, \tag{34}$$

where $\mathbf{C}_D$ is a diagonal matrix whose coefficients are given by

$$C_{Dnn} = \varphi_n^{\mathrm{T}}\mathbf{c}\varphi_n = 2\xi_n\omega_n \tag{35}$$

and $\mathbf{C}_F$ is a matrix whose diagonal coefficients are null with the non-diagonal terms given by

$$C_{Fnp} = \varphi_n^{\mathrm{T}}\mathbf{c}\varphi_p \quad (C_{Fnp} = 0 \text{ if } n = p). \tag{36}$$

The term which accounts for pseudo-forces due to non-proportional damping can be obtained by following a procedure similar to that developed when non-linearities were considered. When non-linear behaviour is considered together with non-proportional damping, the following equation for the kth iteration can be written

$$\mathbf{Y}_j^{(k)} = \mathbf{Y}_{nj}^{(k)} + Y_{0j}\mathbf{1},$$

$$\mathbf{Y}_{nj}^{(k)} = \frac{1}{N}\mathbf{e}_j\left(\mathbf{P}_{nj} - F_{0j}\mathbf{1} + \frac{\dot{Y}_j}{\Delta t}\boldsymbol{\delta} + \sum_{p=1}^{NGL} K_{Njp}\mathbf{Y}_{np}^{(k-1)} - \sum_{p=1}^{NGL} C_{Fjp}\dot{\mathbf{Y}}_{np}^{(k-1)}\right) \tag{37}$$

8. NUMERICAL EXAMPLES

8.1. PRELIMINARY REMARKS

In order to carry out a numerical analysis one has *a priori* to make a decision about the values of DFT parameters which lead to accurate numerical results. Some guidelines may be recommended; however, an optimal choice of such parameters can only be achieved if one has experience in the problem being analyzed.

8.1.1. *Extended period* T_p

The period either for linear analyses or for each segment of non-linear analysis must be large enough to prevent a periodic behaviour of the time-history of displacements. As $\mathbf{e}$ is a lower triangular matrix, the extended period T_p is not related to time duration of external loads, rather it must be such that the first column of matrix $\mathbf{e}$ is accurately computed (note that $\mathbf{e}$ is a Toeplitz matrix). In fact, T_p depends only on $\mathbf{m}$, $\mathbf{c}$ and $\mathbf{k}$, and must be such that $g(T_p)$ is small, $g(t)$ being the unit impulse response function which for an s.d.o.f. system is given by

$$g(t) = \frac{1}{\omega\sqrt{1-\xi^2}}\,\mathrm{e}^{-\omega\xi t}\sin(\omega t\sqrt{1-\xi^2}). \tag{38}$$

Given a tolerance α, T_p can be estimated from

$$\mathrm{e}^{-\xi T_p \omega} < 10^{\alpha} \tag{39}$$

or

$$T_p > \alpha \frac{\ln(10)}{\xi\omega} \tag{40}$$

where ξ is the damping ratio and ω is the natural frequency.

The authors have obtained accurate results for $\alpha = 2$ and recommend $2 \leqslant \alpha \leqslant 4$.

8.1.2. *Number of sampling points N*

As is usual in DFT analysis the number of sampling points must prevent *aliasing* [10,13], i.e., the sampling interval Δt must be small enough so that

$$\frac{1}{2\Delta t} > f_N, \tag{41}$$

where f_N is the Nyquist frequency. The sampling interval is $\Delta t = T_p/(N-1)$.

8.1.3. *The parameter S*

This parameter only indicates the number of time points at which the response is to be computed. As such it has no influence either on accuracy or on stability of the algorithm. However, S has great influence on the cost of the analysis mainly for non-linear structural systems. S being too small introduces unnecessary segments, whereas large values of S lead to unnecessary computations of the response beyond a segment.

8.1.4. *Tolerance ε of the pseudo-force iterative process*

In all examples analyzed here the authors have adopted $\varepsilon = 1\%$.

8.1.5. *Time-domain analyses*

In order to verify the accuracy of the frequency-domain (FD) method discussed here, time-domain analyses were also carried out for each of the following examples. The time-domain approach is based on the Newmark scheme, as presented by Weaver and Johnston [14], with the parameters γ and β taken as $\gamma = 1/2$ and $\beta = 1/6$. In fact, this choice leads to the linear acceleration method. Except when mentioned, the time-domain analyses employ the same time-step adopted in the frequency-domain analyses. The CPU time of the time-domain analyses were lower than those of the frequency domain analyses. For the applications presented here, this is not an important parameter as no analysis took more than 2 s (overall computer time) in a micro-computer Pentium II 450 MHz. CPU computer time is not a parameter to be concerned with, as time- and frequency-domain approaches are not meant to be competitive, rather they are complementary to one another [10]. There are many dynamic problems which can be solved either by time- or frequency-domain procedures; in this case, the cheaper one should be chosen. However, time-domain approaches do not apply when the dynamic system properties are frequency dependent: in this case one is left with no other choice but to use frequency-domain methods. One such case where time-domain approaches cannot be applied is discussed here in application 2, where hysteretic damping was considered for the structure.

8.2. EXAMPLE 1

The s.d.o.f. system shown in Figure 3(a) has mass equal to 17·5 t and a viscous damping coefficient equal to 21 kN s/m. The spring stiffness coefficient is bilinear as shown in Figure 3(b). The natural frequency is 7·07 rad/s and the damping ratio is 8·5%.

The following parameters, related to the implicit Fourier transform algorithm and to the iterative pseudo-force process, were adopted: $N = 2000$, $\Delta t = 0{\cdot}0125$, $S = 120$ and $\varepsilon = 1\%$. For the time-domain analysis, $\Delta t = 0{\cdot}012$.

In the non-linear analysis, one may have to change from the current segment to the subsequent one (see Figure 2) at discrete time values lower than $S\Delta t$ ($S = 120$), in which case the remaining terms of the time response history are not considered.

In the first analysis the system is subjected to the loading time-history shown in Figure 4. Linear and non-linear ImFT and Newmark responses depicted in Figure 5 agree quite well.

Concerning the non-linear analysis, the spring works linearly under tension at the initial stage, reaches later a non-linear phase, subsequently enters into a compressive linear phase, returns to the non-linear phase and finally oscillates linearly until motion stops. Thus, at rest, the spring will have a residual strain (negative in the present analysis).

In order to check the robustness of the ImFT approach, another analysis was carried out where the s.d.o.f. system shown in Figure 3 was excited by a base motion whose input acceleration, depicted in Figure 6, corresponds to the first 4 s of the "El Centro" earthquake.

The time-domain and ImFT results shown in Figure 7 agree quite well. For these analyses, $\Delta t = 0{\cdot}0125$ s. It should be observed that in this analysis the system crosses many times the non-linear threshold.

8.3. EXAMPLE 2

The shear building depicted in Figure 8 is submitted to "El Centro" earthquake base acceleration. The top-floor movement is partially restricted by a discrete viscous damper whose damping constant c is equal to 3·5 MN s/m. This shear building has been analyzed previously by Clough and Penzien [10], who computed the eigenvalues of the correspondent undamped problem.

Three different situations were simulated as described next. In the first analysis, the discrete viscous damper was removed and Rayleigh damping was considered for the structure [10], i.e., $\mathbf{c} = a_0\mathbf{m} + a_1\mathbf{k}$. As this analysis is linear, and the damping matrix is

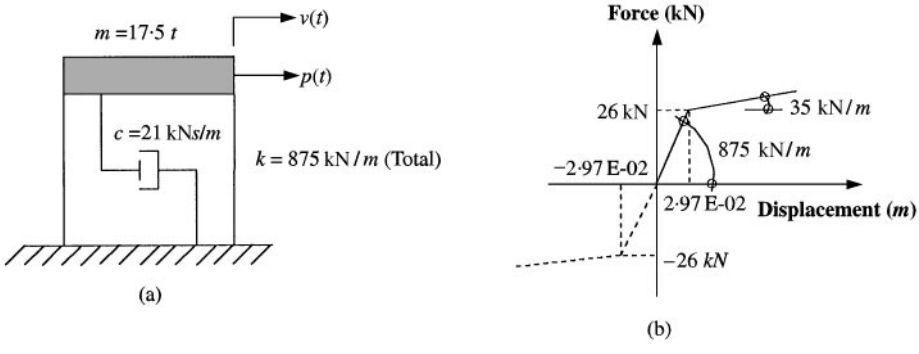

Figure 3. Single-degree-of-freedom shear building: (a) properties; (b) bilinear stiffness coefficient.

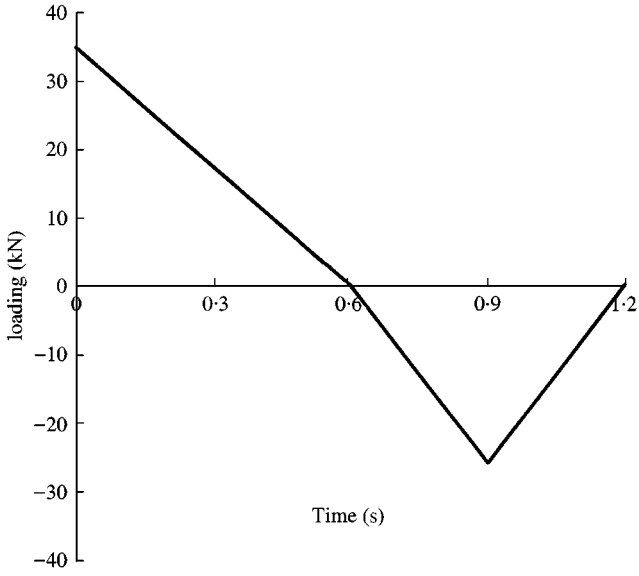

Figure 4. Loading time-history: example 1, first analysis.

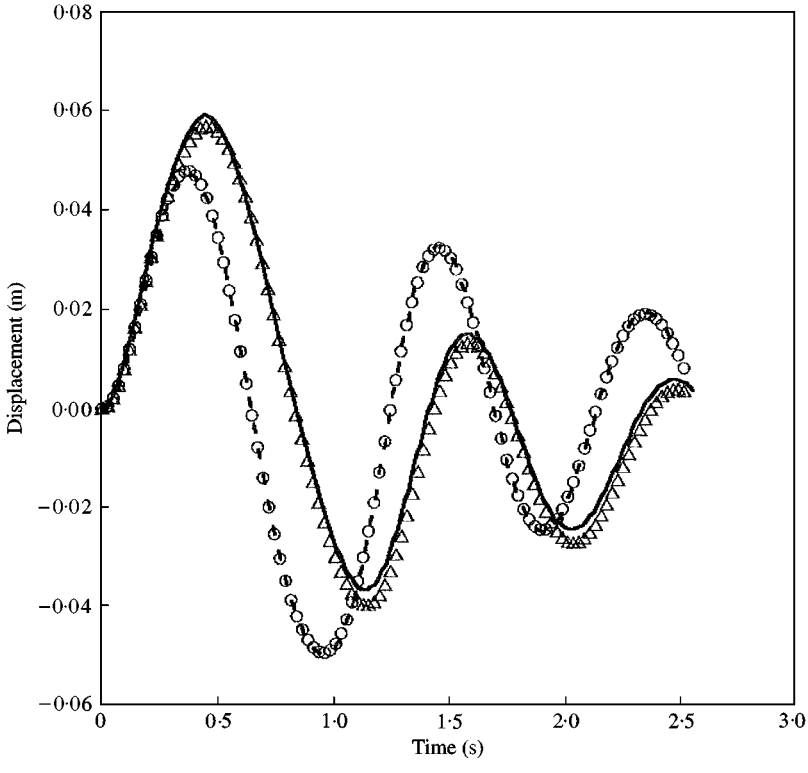

Figure 5. ImFT and Newmark time responses for the s.d.o.f. system subjected to the load depicted in Figure 4: – – – –, linear analysis, ImFT; ○, linear analysis, Newmark; ——, non-linear analysis, ImFT; △, non-linear analysis, Newmark.

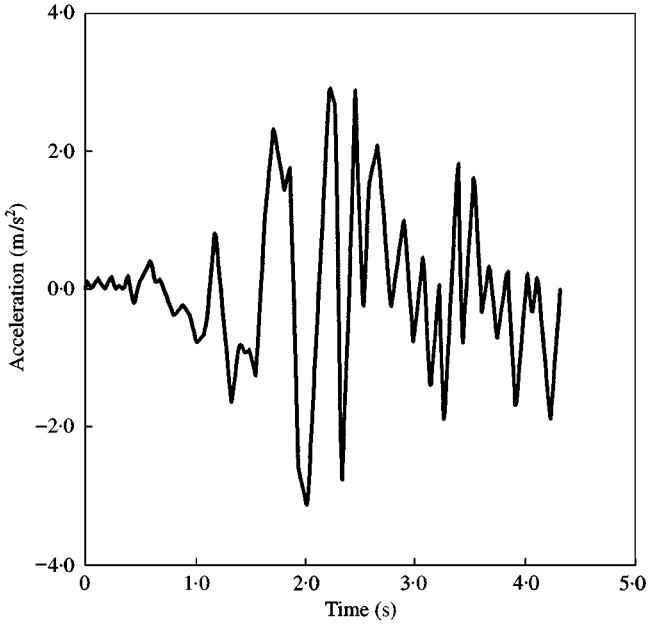

Figure 6. Base acceleration of "El Centro" earthquake.

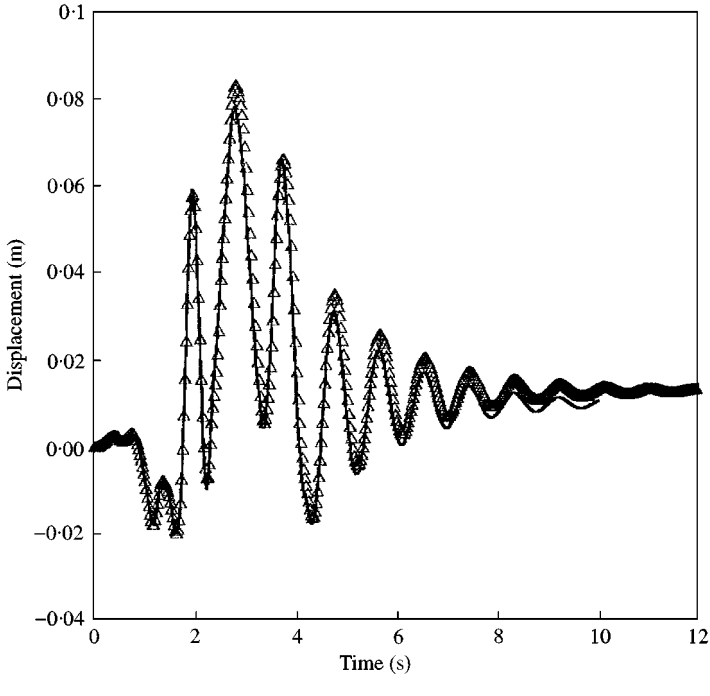

Figure 7. Non-linear ImFT and Newmark time responses for the s.d.o.f. system subjected to "El Centro" earthquake base acceleration: ——, ImFT; △, Newmark.

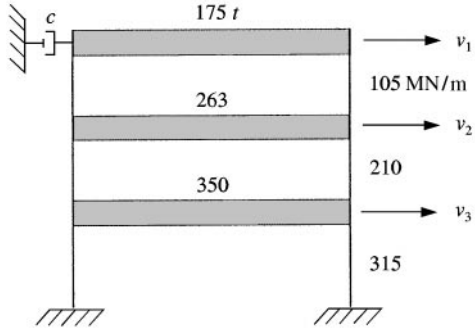

Figure 8. Three-degree-of-freedom shear building.

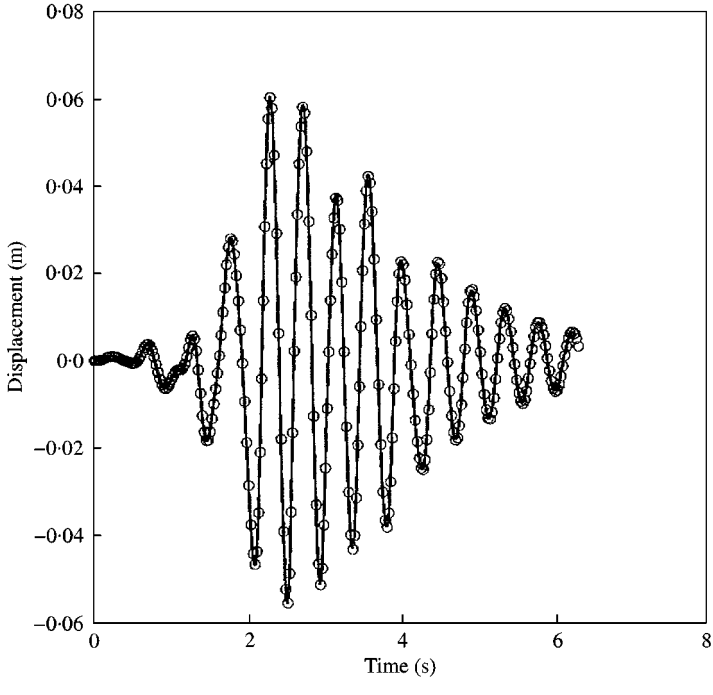

Figure 9. Displacement time-history of the top floor of the shear building depicted in Figure 8 for proportional Rayleigh damping: ——, ImFT; ○, Newmark.

proportional, the analysis is not iterative. Time-histories of the top floor obtained with Newmark and ImFT algorithms, depicted in Figure 9, agree quite well.

Figure 10 shows the time-history of the top-floor displacement of the shear building as shown in Figure 8, i.e., the discrete damper is included in this analysis. Thus, the damping matrix **c** is non-proportional, the modal damping matrix being given by

$$\mathbf{C} = \begin{bmatrix} 2{\cdot}18 & -1{\cdot}65 & 0{\cdot}55 \\ -1{\cdot}65 & 1{\cdot}89 & -0{\cdot}47 \\ 0{\cdot}55 & -0{\cdot}47 & 0{\cdot}96 \end{bmatrix}$$

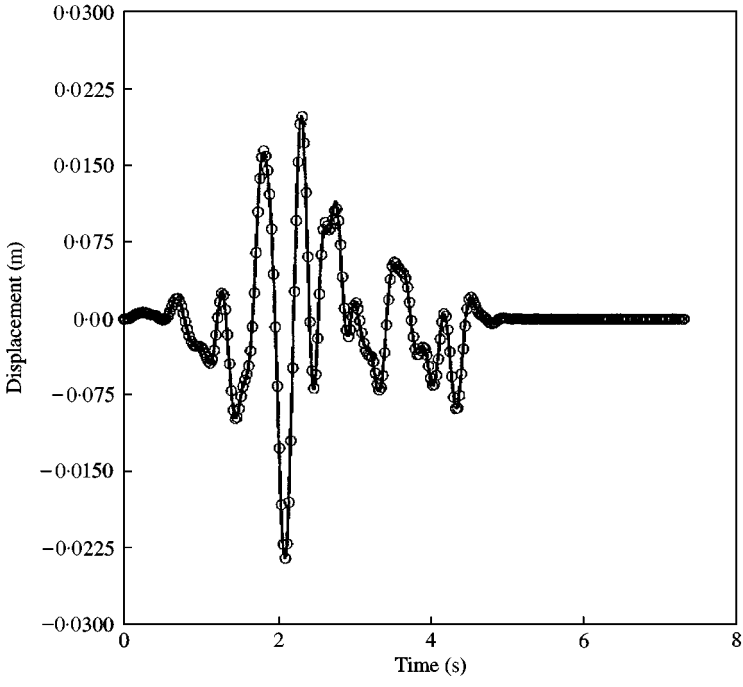

Figure 10. Displacement time-history of the top floor of the shear building depicted in Figure 8 for non-proportional damping: ——, ImFT; ○, Newmark.

The modal system is coupled, as the off-diagonal coefficients of the **C** matrix shown above are not null. The pseudo-force method required four iterations to achieve convergence. Results obtained with the frequency-domain approach (ImFT), for $N = 1000$, and with the Newmark scheme are identical.

A last analysis concerning this three-storey shear building was carried out where the discrete damper was included and hysteretic rather than Rayleigh damping was considered for the structure, the damping ratio being $\xi = 5\%$. The time-history of the top-floor displacement due to the ImFT approach, using Rayleigh and hysteretic damping for the structure, is shown in Figure 11. Results, once again, agree quite well. For all analyses corresponding to this example, $\Delta t = 0{\cdot}0125$ s.

8.4. EXAMPLE 3

The 2 d.o.f. system shown in Figure 12(a) is a simplified model of the structure of a nuclear reactor containment. The masses of the foundation m_f and of the structure m_s are, respectively 10^8 and 3×10^7 kg. The stiffness coefficient of the structure is $k_s = 6 \times 10^{10}$ N/m. The soil behaviour is non-linear, as shown by the load–deflection curve depicted in Figure 12(b). The system is submitted to a horizontal impact load, whose time-history is depicted in Figure 13. The damping coefficient of the soil computed according to Richart *et al.* [15] is $3{\cdot}79 \times 10^9$ Ns/m. Natural frequencies corresponding to modes 1 and 2 are, respectively, equal to 31·26 and 56·33 rad/s and the corresponding damping ratios are, respectively, equal to 0·2824 and 0·1797.

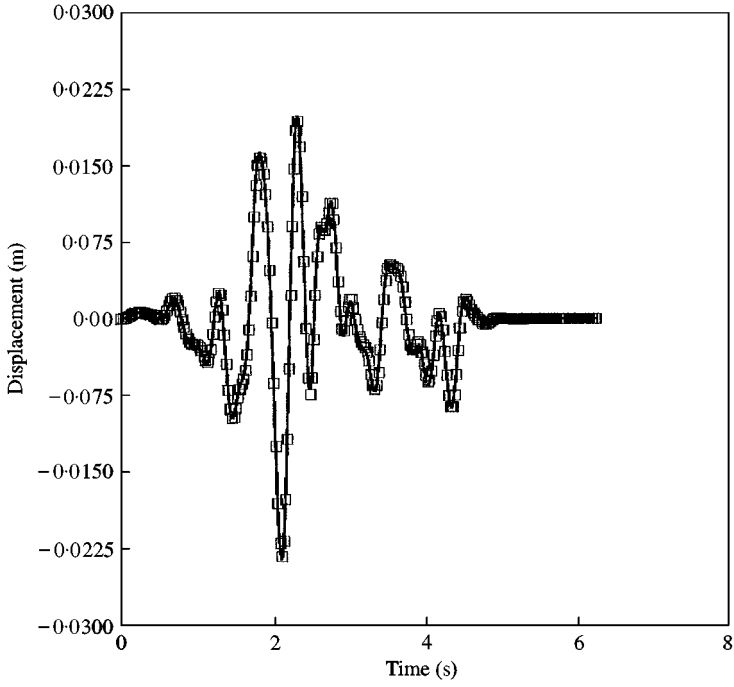

Figure 11. Displacement time-history, obtained with the ImFT, of the top floor of the shear building depicted in Figure 8 for non-proportional damping: ——, Rayleigh damping for the structure; □, hysteretic damping for the structure.

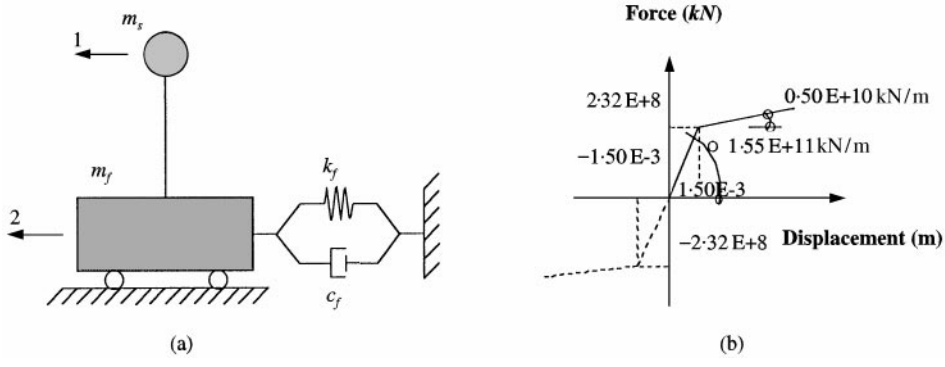

Figure 12. Two-degree-of-freedom nuclear reactor model: (a) 2 d.o.f. system, (b) bilinear stiffness coefficient of the soil.

In this example the following parameters related to the implicit Fourier transform algorithm and to the iterative pseudo-force process were adopted: $N = 1024$, $\Delta t = 0{\cdot}01$ s, $S = 60$ and $\varepsilon = 1\%$.

The time-histories of the foundation displacement corresponding to Newmark ($\Delta t = 0{\cdot}005$ s) and ImFT algorithms are depicted in Figure 14, considering the soil behaviour to be linear or non-linear. It must be highlighted that in the ImFT non-linear model the iterative expression (37) has been employed, i.e., the mechanical system is

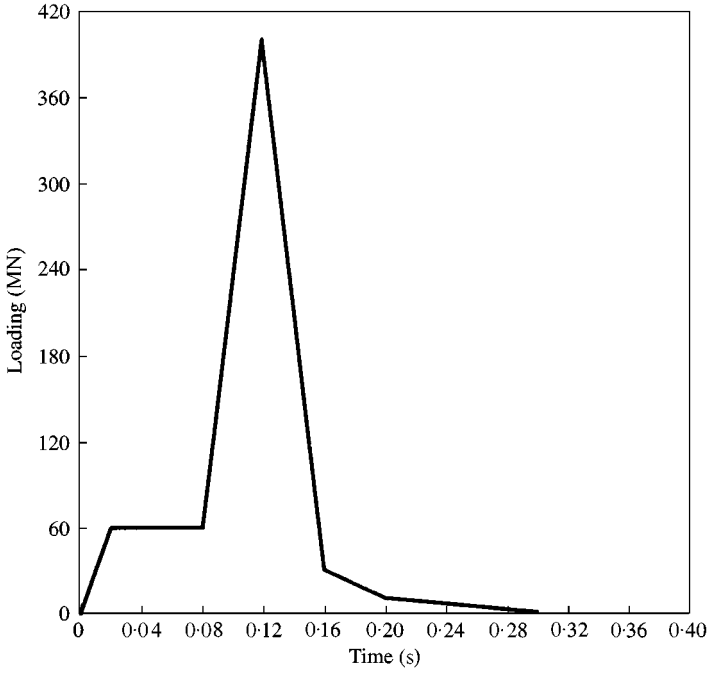

Figure 13. Impact over mass m_s for the nuclear reactor model.

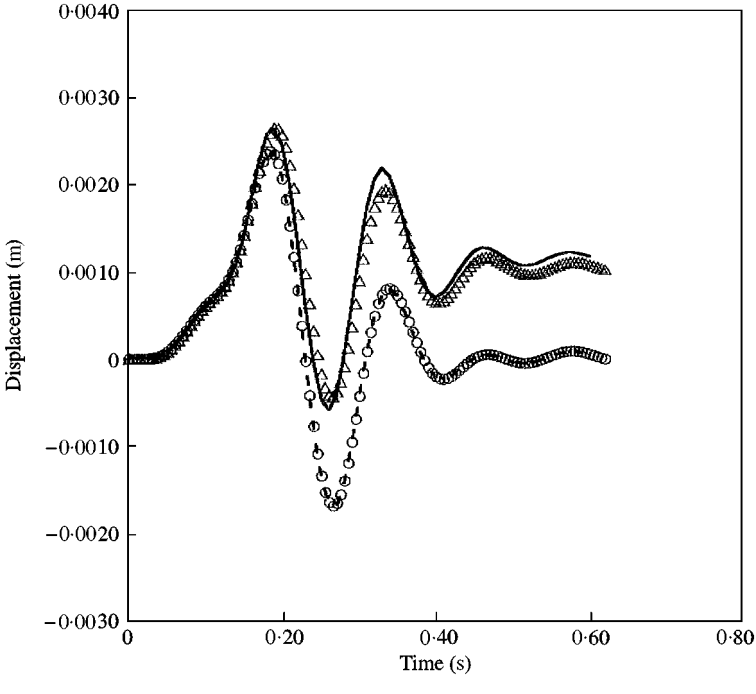

Figure 14. Foundation displacement time-history for the nuclear reactor model: – – – –, linear analysis, ImFT; ○, linear analysis, Newmark; ——, non-linear analysis, ImFT; △, non-linear analysis, Newmark.

non-linear with non-proportional damping. Results of time-domain and ImFT algorithms agree quite well, giving residual displacements quite close. The overall computer time for the ImFT procedure was equal to 1 s and, for the Newmark scheme, was lower than 1 s.

9. CONCLUSIONS

This work presented a new robust frequency-domain formulation, which can be used to find time responses of either linear or non-linear structural systems, having non-proportional damping characteristics.

Time-history of displacement for 1 d.o.f. systems was obtained via the matrix formulation of the discrete Fourier transform, denoted here by implicit Fourier transform (ImFT). One important property of the ImFT matrix **e**, the causality property, has been discussed here. It was shown that one need not consider the $(N \times N)$ terms of **e** when only the first S $(S < N)$ terms of the time response history are required, i.e., a reduced lower triangular **e** $(S \times S)$ implicit discrete Fourier matrix can be considered, leading to substantial computer time savings.

In the procedure presented here for linear m.d.o.f. systems the mode superposition method was employed. The final system is uncoupled and the same frequency domain algorithm used for the 1 d.o.f. system could be employed. When the system is non-linear, with non-proportional damping, the system of equations in modal co-ordinates is not uncoupled any more. In this case, terms responsible for coupling are transferred to the r.h.s. of the system of equations, being considered as pseudo-forces. An iterative procedure arises, in which the l.h.s. of the final system of equations is uncoupled, and thus the modal matrix needs to be computed only once.

The pseudo-force method together with the correct consideration of initial conditions for m.d.o.f. systems led to a correct modelling in the frequency domain of the three examples discussed here; ImFT results were quite close to those arising from a time-domain procedure based on the Newmark scheme.

It is important to notice that when CPU computer time is concerned, time-domain approaches (e.g., Newmark, Wilson θ, central differences, etc. [14, 16]) are cheaper in many applications. However, time- and frequency-domain approaches are not meant to be competitive, rather they are complementary to one another. Time-domain procedures do not apply when dynamic properties have to be defined in the frequency-domain, as illustrated by the third analysis of the second example (see Figure 11) where hysteretic damping was considered for the structure. Naturally, for the range of problems to which time- and frequency-domain approaches apply equally, one will choose the cheapest one. In fact, computer time is critical when the number of the d.o.f. is too large, otherwise computer cost is not relevant.

As a final remark, it should be observed that ImFT computational costs could be substantially reduced if modal truncation procedures are employed.

REFERENCES

1. J. D. KAWAMOTO 1983 *Research Report R*83-5, *MIT*, *Dept. of Civil Eng.* Solution of nonlinear dynamic structural systems by a hybrid frequency-time domain approach.
2. A. APRILE, A. BENEDETTI and T. TROMBETTI 1994 *Earthquake Engineering and Structural Dynamics* **3**, 363–388. On non-linear dynamic analysis in the frequency domain.
3. T. ITOH 1973 *Earthquake Engineering and Structural Dynamics* **2**, 47–57. Damping vibration mode superposition method for dynamic response analysis.

4. H. CHEN and R. L. TAYLOR 1987 *Numerical Methods in Engineering Theory and Applications* (*NUMETA* 87) t5/1 **2**, 1–10. Properties and solutions of eigensystems of non-proportionally damped linear dynamic systems.
5. C. J. CHANG and B. MOHRAZ 1990 *Computers and Structures* **36**, 1067–1080. Modal analysis of non-linear systems with classical and non-classical damping.
6. A. M. CLARET and F. VENANCIO-FILHO 1991 *Earthquake Engineering and Structural Dynamics* **20**, 303–315. A modal superposition pseudo-force method for dynamic analysis of structural systems with non-proportional damping.
7. R. S. JANGID and T. K. DATTA 1993 *Earthquake Engineering and Structural Dynamics* **22**, 723–735. Spectral analysis of systems with non-classical damping using classical mode superposition technique.
8. F. VENANCIO-FILHO and A. M. CLARET 1992 *Computers and Structures* **42**, 853–855. Matrix formulation of the dynamic analysis of SDOF in frequency domain.
9. W. G. FERREIRA, A. M. CLARET, and F. VENANCIO-FILHO 1997 *Ibero-Latin American Congress of Computational Methods in Engineering* (XVIII *CILAMCE*) **2**, 815–820. The treatment of initial conditions in frequency-domain dynamic analysis.
10. R. W. CLOUGH and J. PENZIEN 1993 *Dynamics of Structures.* New York: McGraw-Hill, second edition.
11. W. G. FERREIRA 1998. *D.Sc. Thesis* (*in Portuguese*), *COPPE, Federal University of Rio de Janeiro, Brazil*. Non-linear dynamic analysis of structural systems with non-proportional damping in the frequency domain.
12. W. WEAVER, S. P. TIMOSHENKO and D. H. YOUNG 1989 *Vibration Problems in Engineering*. New York: John Wiley and Sons, fifth edition.
13. M. PAZ 1997 *Structural Dynamics — Theory and Computations.* New York: Chapman and Hall, fourth edition.
14. W. WEAVER JR. and P. R. JOHNSTON 1987 *Structural Dynamics by Finite Elements.* Englewood Cliffs, NJ: Prentice-Hall.
15. F. E. RICHART JR, R. D. WOODS and J. R. HALL JR. 1970 *Vibrations of Soils and Foundations.* Englewood Cliffs, NJ: Prentice-Hall.
16. K. BATHE 1996 *Finite Element Procedures.* Englewood Cliffs, NJ: Prentice-Hall.